Czech Technical University in Prague
Faculty of Nuclear Sciences and Physical Engineering

RESEARCH WORK

The Asymptotic Behaviour of the Heat Equation in Twisted Waveguides

Gabriela Malenová

I would like to thank my supervisor David Krejčiřík for introducing me to the concept of self-similarity transformation and other theoretical parts, I also appreciate his kind support, valuable guidance and carefuly corrections which enabled me to write this work. I also thank to the consultant Miloš Tater who provided me the assistance in numerics.

Prohlášení

Prohlašuji, že jsem svou práci vypracovala samostatně a použila jsem pouze podklady uvedené v přiloženém seznamu.

Declaration

I declare that I wrote my research work independently and exclusively with the use of cited bibliography.

Praha, 2011

Gabriela Malenová

Název práce:
Asymptotické chování rovnice vedení tepla ve zkroucených vlnovodech

Autor: Gabriela Malenová

Obor: Matematické inženýrství

Druh práce: Rešeršní práce

Vedoucí práce: Mgr. David Krejčiřík, Ph.D.
ÚJF AV ČR, Řež

Abstrakt: Uvažujeme rovnici vedení tepla ve zkrouceném vlnovodu. Z teorie je známo, že míra útlumu pologrupy klesá, pokud je vlnovod zkroucený. Naším cílem je podpořit tato data numerickými výsledky. Vhodné metody jsou vyvinuty v prostředí Wolfram Mathematica.

Klíčová slova: vlnovod, rovnice vedení tepla, míra útlumu, zkroucení

Title:
The asymptotic behaviour of the heat equation in the twisted waveguides

Author: Gabriela Malenová

Abstract: We consider the heat equation in the twisted waveguides. As known from the theory, the decay rate of the heat semigroup increases if the waveguide is twisted. Our goal is to support this data by numerical results. The suitable methods are developed in the Wolfram Mathematica environment.

Key words: waveguide, heat equation, decay rate, twist

Contents

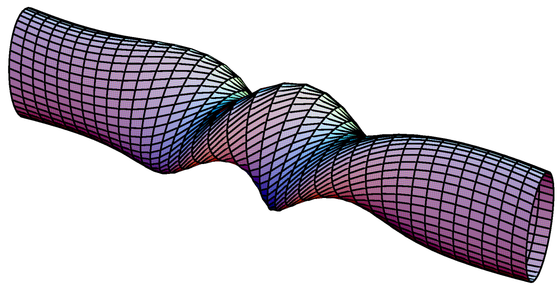

Figure 1: Twisted waveguide.

1 Introduction

The time evolution profile of some quantity such as heat or chemical concentration within an object depends upon the conduction to its boundaries. This is mathematically described by the *heat equation*

$$u_t - \Delta u = 0, \tag{1}$$

with imposed boundary conditions. Physically, the Dirichlet condition on the boundary describes the quantity distribution within the object while such a substance is of a high capacity and of zero temperature/concentration on the boundary. Neumann boundary condition gives evolution of the quantity distribution of a medium surrounded by a perfect insulator. (1) also represents the simplest version of the stochastic Fokker-Planck equation describing the Brownian motion in the object which is normally reflected on the Neumann boundary trace and killed on the Dirichlet trace [7].

In present work, the heat equation in the inifinite tube Ω_θ, called *waveguide*, is considered. We are introducing a problem, how the solution depends on the geometrical properties, namely what happens if the waveguide were *twisted*. The idea behind this research goes back to the quantum waveguides and the solution of Schrödinger equation. On the Figure 1, there is an example of a three-dimensional twisted waveguide. More precisely, the section 2.2 is devoted to them.

More details about the two-dimensional waveguides are involved in the section 4.3. An example of such a waveguide is displayed on the Figure 2.

Noteworthy progress has been made in the theory of geometrically shaped quantum waveguides from the very beginning in 90's since Exner and Šeba published their crucial article [5]. They postulated that the bending of a quantum waveguide represents an effective attractive potential perturbation in the sense that bound states under the threshold energy are generated.

Other types of geometrical deformations, such as twisting, has been thoroughly investigated later, from this perspective the breakthrough article by T. Ekholm, H. Kovařík and D. Krejčiřík [3] presents a connection of spectral stability to the Hardy inequalities. The authors showed that the twist causes

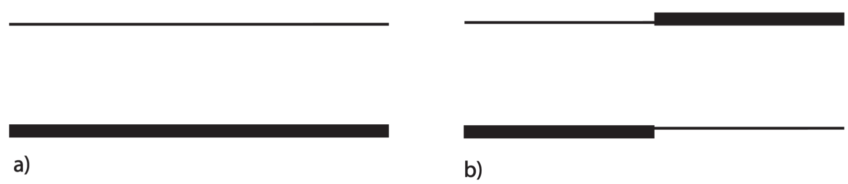

Figure 2: a) An untwisted and b) a twisted waveguide. The bold line denotes the Dirichlet and the thin line the Neumann boundary condition.

notwithstanding a repulsive perturbation which suppresses existence of eigenstates below the essential spectrum, in other words the Hamiltonian is subcritical. A survey article [6] on comparing these two deformations has been published.

The natural question arises whether the twist influences other processes beside Schrödinger equation as well. The first connection between Hardy inequalities in the twisted three-dimensional waveguide Ω_θ and heat equation (1) subject to Dirichlet boundary condition in $\partial\Omega_\theta$, has been investigated in [8]. In the article a discovery was made that the decay rate of the heat equation increases if the twist is considered. More precisely, the decay rate $\gamma(\Omega_\theta)$ may be defined in the fashion of the heat equation solution $u(x,t)$ (1) as

$$\gamma(\Omega_\theta) := \sup\left\{\gamma \,\middle|\, \exists C,\ \forall t,\ u_0 \|u(t)\| \leq C(1+t)^{-\gamma} e^{-E_1 t} \|u_0\|_K\right\}, \qquad (2)$$

$\forall u_0 \in L^2(\Omega_\theta, K)$, where E_1 is the threshold energy of the Dirichlet Laplacian $-\Delta_D^\omega$ spectrum on the cross-section ω and $\|.\|_K$ indicates the norm in the weighted space

$$L^2(\Omega_\theta, K), \quad K(x) := e^{x_1^2/4}.$$

D. Krejčiřík and E. Zuazua stated the value of $\gamma(\Omega_\theta)$ as follows:

$$\gamma(\Omega_\theta) \begin{cases} = 1/4 & \text{if } \Omega_\theta \text{ is untwisted,} \\ \geq 3/4 & \text{if } \Omega_\theta \text{ is twisted.} \end{cases}$$

By using the same approach the authors estimated in [7] the above asymptotical decay rate in the two-dimensional Dirichlet-Neumann waveguide.

The main goal of present work is to support this data numerically. Some procedures in Wolfram Mathematica environment are developed, which agree with the statement that decay rate increases as the twist is imposed. Unfortunately, they seem to be unstable and are not giving the correct limit behaviour so far.

In the last section some related results are presented. To get familiar with the spectral method, we solved the heat equation in MATLAB on the finite area either in one or in two dimensions. The moving frame of the heat equation time evolution in the finite rectangle is provided there.

2 Preliminaries

Let us first recall some basic facts about twisted waveguides and heat equation. In order to carry out the time-evolution of its solution, one should introduce some parts of semigroup theory as well.

2.1 Semigroup theory

Semigroup is a mathematical structure where the associative binary operation on a set is defined. It naturally generalizes the group, since every element does not have to have an inverse. More specifically [12]:

Definition 1. $\{S(t), t \geq 0\}$ is a *linear contraction semigroup* if $S(t) : \mathcal{H} \to \mathcal{H}$ is a linear contraction

$$\|S(t)\| \leq 1$$

for each $t \geq 0$ and

$$S(t+\tau) = S(t)S(\tau) \quad \text{for } t, \tau \geq 0, \tag{3}$$

$$S(0) = I, \tag{4}$$

$$S(.)x \in C([0,\infty), \mathcal{H}) \quad \text{for each } x \in \mathcal{H}, \tag{5}$$

$\|.\|$ here denoting the operator norm.

Definition 2. Let $\mathcal{H}$ be the Hilbert space, D a subspace, and $A : D \to \mathcal{H}$ an unbounded linear operator. The *Cauchy problem* of the evolution equation

$$u'(t) + Au(t) = 0, \quad t > 0, \tag{6}$$

is to find a solution $u \in C([0,\infty), \mathcal{H}) \cup C^1((0,\infty), \mathcal{H})$ such that $u(t) \in D(A)$ for $t > 0$ and $u_0 \in \mathcal{H}$ is prescribed.

The operator $-A$ can be recovered from semigroup as the right derivative in $t = 0$:

$$-Au_0 = \lim_{t \to 0_+} \frac{u(t) - u(0)}{t}. \tag{7}$$

Definition 3. The generator of linear contraction semigroup is the operator $B : D(\mathcal{H}) \to \mathcal{H}$ defined through

$$Bu := \lim_{t \to 0_+} t^{-1}(S(t) - I)\, u,$$

where $u \in D(B)$ iff this limit exists.

Suppose A be an self-adjoint operator in some Hilbert space $\mathcal{H}$. Then, according to spectral theorem [1], A can be expressed as an integral of projections:

$$A := \int_{\sigma(A)} \lambda \, dP(\lambda),$$

where $P(\lambda)$ is a projection valued measure. The family of projection operators $P(\lambda)$ is called *resolution of the identity* for A. Then any function of A may be assigned as

$$f(A) := \int_{\sigma(A)} f(\lambda)\, dP(\lambda).$$

For f being the exponential of A we conclude with

$$\exp(A) = \int_{\sigma(A)} e^{\lambda}\, dP(\lambda).$$

Requiring an operator A being bounded, the exponential operator may be defined in $\mathcal{L}(\mathcal{H})$ as

$$\exp(A) := \sum_{n=0}^{\infty} \frac{A^n}{n!}. \tag{8}$$

We take advantage of this notation for the unbounded operators exponential as well. The detailed procedure may be found in the proof of Hille-Yosida Theorem in [4].

Theorem 2.1. Hille-Yosida. *Let A be a closed, densely-defined linear operator on X. Then A is the generator of the contraction semigroup $\{S(t) : t \geq 0\}$ if and only if*

$$(0, \infty) \subset \rho(A), \quad \textit{and} \quad \|R_\lambda\| \leq \frac{1}{\lambda} \quad \textit{for} \quad \lambda > 0.$$

Proof. Firstly, we regularize the not necessarily unbounded operator A as

$$A_\lambda := -\lambda I + \lambda^2 R_\lambda = \lambda R_\lambda A,$$

where λ belongs to the $\rho(A)$, *resolvent set of* A, provided the operator

$$\lambda I - A : D(A) \to X$$

is on-to-one and onto, and $R_\lambda : X \to X$ denotes the *resolvent operator* defined by

$$R_\lambda u := (\lambda I - A)^{-1} u.$$

According to the closed graph theorem [D.3 [4]] the resolvent operator is a bounded linear operator, out of which we conclude that the exponential of A_λ exists in the sense of (8) and we are allowed to define a semigroup $S_\lambda(t)$ as

$$S_\lambda(t) := e^{tA_\lambda} = e^{-\lambda t}\, e^{\lambda^2 t R_\lambda} = e^{-\lambda t} \sum_{k=0}^{\infty} \frac{(\lambda^2 t)^k}{k!}\, R_\lambda^k.$$

By claiming $\|R_\lambda\| \leq \lambda^{-1}$ we may deduce

$$\|S_\lambda(t)\| \leq 1,$$

thus $\{S_\lambda(t) : t \geq 0\}$ is a contraction semigroup and is easy to check its generator is A_λ, with $D(A_\lambda) = X$. Consequently,

$$S(t)u := \lim_{\lambda\to\infty} S_\lambda(t)u,$$

exists for each $t \geq 0$, $u \in D(A)$. It remains to show that A is the generator of $\{S(t) : t \geq 0\}$. Indeed, the extended proof is performed in [4]. $\square$

In the case A has a complete orthonormal system $\{u_n\}_{n=1}^{\infty}$ of eigenvectors, i. e. the spectrum is purely discrete

$$Au_n = \lambda_n u_n,$$

we may recall Galerkin method [7.1, [4]] for converting a continuous operator problem (such as a differential equation) to a discrete problem. It may be shown that

$$Au = \sum_{n=1}^{\infty} \lambda_n \langle u_n, u\rangle u_n,$$

for all $u \in D(A)$ iff $\sum |\lambda_n \langle u_n, u\rangle|^2 < \infty$. Thus the exponential of A is defined as following:

$$e^{-At}u := \sum_{n=1}^{\infty} e^{-\lambda_n t}\langle u_n, u\rangle\, u_n, \quad \forall t \geq 0.$$

Thereby for the family of operators

$$S(t) = \exp(-tA).$$

in $\mathcal{L}(\mathcal{H})$, where $t \geq 0$, holds

$$\frac{d}{dt}S(t) = -AS(t).$$

Hence

$$u(t) = S(t)u_0 \tag{9}$$

is the solution of the *Cauchy problem* with $u(0) = u_0$.

Let $\tilde{A}$ be the Fridriech's extension [1] of an operator A. Then the equation $u' + \tilde{A}u = 0$ with $u(0) = u_0$ is a *generalized problem* to the Cauchy problem (6). The solution $u = u(t)$ is called *mild (generalized) solution.* The following proposition says how the self-adjoint extension looks like. The proposition as well as the proof is findable in [12].

Proposition 2.2. *Let a linear operator $A \in L(D, \mathcal{H})$ be closed and accretive, D dense in $\mathcal{H}$, and assume for every $u_0 \in D$ there exists a solution $u \in C^1([0,\infty), \mathcal{H})$ of (6) on $t \geq 0$ with $u(0) = u_0$. Construct $\{S(t), t \geq 0\}$ as above, so $u(t) = S(t)u_0,\ t \geq 0$. Then $\{S(t), t \geq 0\}$ is a linear contraction semigroup on $\mathcal{H}$ whose generator is an extension of $-A$.*

Proof. A is accretive, therefore the Cauchy problem (6) has at most one solution. While D is dense in $\mathcal{H}$ each $S(t)$ has a unique extension to a contraction on $\mathcal{H}$. Thus we are able to construct $\{S(t), t \geq 0\}$ according to Definition 3. Setting $u_0 \in D$ and recalling (7) we have

$$S(t)u_0 - u_0 = u(t) - u_0 = \int_0^t u' = -\int_0^t Au(s)ds, \quad t > 0.$$

Since the integrand is continuous on $[0, \infty)$ we arrive at

$$Bu_0 = -Au_0.$$

□

Function $u(t) := S(t)u_0$, for all $t \geq 0$ and u_0 fixed, is called *possible process*. According to the semigroup property (3) it follows, that

$$u(t + \tau) = S(t)u(\tau), \quad \forall t \text{ and fixed } \tau.$$

This allows interpretation:

- *Causality.* The state of the system for $t > \tau$ is uniquely determined by the state $u(\tau)$.
- *Homogenity.* If $t \mapsto u(t)$ is a possible process $\forall t \geq 0$, then so is the process $t \mapsto u(t + \tau)$ for all $t \geq 0$ and fixed τ.
- *Irreversibility.* If $t \mapsto u(t)$ is a possible process, we can not achieve the initial state by reversing the time, $t \mapsto u(-t)$ is not possible process.

2.2 Waveguides

One may imagine a waveguide as an infinite tube. Bending and twisting are examples of geometrical deformations of the waveguides which have influence on the physical properties as well. We will consider the latter one (see Figure 1), bending properties has been intensively studied in the last decades, see the breakthrough article [5].
More specifically, the untwisted waveguide is denoted by $\Omega_0 := \mathbb{R} \times \omega$, where $\omega \in \mathbb{R}^2$ is a non-circular cross-section. The twisted waveguide Ω_θ is created from the untwisted one by rotating ω around the x_1-axis with the non-constant angle $\theta : \mathbb{R} \to \mathbb{R}$. At the same time, ω is not rotationally symmetric with respect to the origin in $\mathbb{R}^2$ [8].
Mathematically, the waveguide properties are performed by the Dirichlet Laplacian $-\Delta_D^{\Omega_\theta} : L^2(\Omega_\theta) \to L^2(\Omega_\theta)$. To avoid difficulties with the operator domain, it is more convenient to work instead of Laplacian with its associated quadratic form $\psi \mapsto \|\nabla\psi\|^2$ with the domain $\mathcal{D}(\Omega_\theta) := H_0^1(\Omega_\theta)$.

Both the twisted and the untwisted operators $-\Delta_D^{\Omega_\theta}$ and $-\Delta_D^{\Omega_0}$ have the same spectrum:

$$\sigma(-\Delta_D^{\Omega_\theta}) = \sigma_{\text{ess}}(-\Delta_D^{\Omega_\theta}) = [E_1, \infty),$$

where E_1 is the lowest eigenvalue of the spectrum of Dirichlet Laplacian $-\Delta_D^{\omega}$ on the cross-section.

The difference, however, lies in the existence of the so-called *Hardy inequality* in the twisted case [3]:

$$-\Delta_D^{\Omega_\theta} - E_1 \geq \rho,$$

ρ is a positive function which decays at the infinity. Such an inequality does not change the spectrum of the operator, but it makes the operator resistant to generating eigenvalues below the essential spectrum by a small potential perturbations. Indeed, eigenvalues below the essential spectrum, so-called *bound states*, occur for the untwisted Dirichlet Laplacian for arbitrary small attractive potentials. This does not happen in the twisted case, the validity of the Hardy inequality implies the absence of bound states. Such an operator is called *subcritical,* while the untwisted Laplacial is *critical.*

Hardy inequalities for special potential have been studied in [3]. The authors have shown that

$$-\Delta_D^{\Omega_\theta} - E_1 \geq \frac{c_H}{1+x_1^2},$$

where $c_H = c_H(\dot{\theta}, \omega) \geq 0$ is positive if and only if Ω_θ is twisted. Some more quantitative results about c_H are presented in [9].

2.3 Heat equation

Heat equation is a parabolic partial differential equation. It is designed as

$$u_t(x,t) - \Delta u(x,t) = 0 \quad \text{on } \Omega_\theta \times \mathbb{R}_+, \tag{10}$$

subject to Dirichlet boundary condition on $\partial\Omega_\theta \times \mathbb{R}_+$. The initial state is denoted $u(x,0) = u_0(x)$ on Ω_θ.

It is easy to see that the heat equation is a Cauchy problem (6) where A is the Friedrich's extension of $A' := -\Delta$ and $D(A') := C_0^\infty(\Omega_\theta)$. In other words, $A := -\Delta_D^{\Omega_\theta}$ with $D(A) := \{u \in H_0^1(\Omega_\theta) : \Delta u \in L^2(\Omega_\theta)\}$. From the semigroup theory it follows that $\forall u_0 \in L^2(\Omega_\theta)$ there exists *uniquely determined* generalized solution of the heat equation.

Proof. (Uniqueness) Let $u, v : \mathbb{R}_+ \to L^2(\Omega_\theta)$; u, v be the $C^1([0,\infty))$ solutions of (6). Let us define a new function

$$w(t) := u(t) - v(t),$$

which also satisfies (6), since $w' + \Delta w = u' - v' + \Delta u - \Delta v = 0$. This implies $w(0) = 0$ because the initial conditions are the same. Then

$$\frac{d}{dt}\langle w(t), w(t)\rangle = 2\langle w'(t), w(t)\rangle = 2\langle \Delta w(t), w(t)\rangle \leq 0, \quad \forall t \geq 0.$$

The inequality follows from the fact, that $-\Delta$ is a positive operator. Consequently, the inequality can be replaced by equal sign.

Using the initial condition $w(0) = 0$ we get

$$\langle w(t), w(t) \rangle = 0,$$

what implies $w(t) = 0, \quad \forall t \geq 0$. This leads to a contradiction $u(t) = v(t)$ for $t \geq 0$, indeed, the solution is unique. $\square$

Recalling the notation for the Hamiltonian in the twisted waveguide using above, we find the solution of (10) in the form

$$u(x,t) = e^{\Delta_D^{\Omega_\theta} t} u_0(x), \tag{11}$$

where $e^{\Delta_D^{\Omega_\theta} t} : L^2(\Omega_\theta) \to L^2(\Omega_\theta)$ is the semigroup operator associated with the Laplacian $-\Delta_D^\theta$.
It follows from the spectral mapping theorem that

$$\|e^{\Delta_D^{\Omega_\theta} t}\|_{L^2(\Omega_\theta) \to L^2(\Omega_\theta)} = e^{-E_1 t}.$$

3 Asymptotic behaviour

3.1 Decay rate

In order to get more information about the long-time behaviour of the heat equation which we are interested in, we define a new quantity to measure the asymptotics, called additional (polynomial) *decay rate* of the semigroup. At first, we restrict the class of initial data on weighted space

$$L^2(\Omega, K), \quad K(x) := e^{x_1^2/4},$$

in other words, the initial data are required to be sufficiently rapidly decaying at the infinity of the tube. Then the decay rate is defined:

$$\gamma(\Omega_\theta) := \sup \left\{ \gamma \mid \exists C_\gamma > 0, \forall t \geq 0, \left\| e^{(\Delta_D^{\Omega_\theta} + E_1)t} \right\|_K \leq C_\gamma (1+t)^{-\gamma} \right\}, \tag{12}$$

where $\|.\|_K : L^2(\Omega, K) \to L^2(\Omega)$.
The striking result which is presented in [7] yields:

Theorem 3.1. *We have $\gamma(\Omega_\theta) = 1/4$ if Ω_θ is untwisted, while $\gamma(\Omega_\theta) \geq 3/4$ if Ω_θ is twisted.*

Thus the decay rate for the twisted case possesses the increment about $1/2$, one can imagine this physically as the heat distribution feathering away faster in the twisted than in the untwisted case.
The proof is carried out by the authors in [7]. We just outline the idea of the extensive and rigorous proof provided there. For this we need to introduce the self-similarity transformation.

3.2 Self-similarity transformation

Motivation: The twisted as well as bent 3-dimensional waveguide can be approximated in such a manner that the cross-section diminishes, thus the tube can be geometrically approximated by the string. The natural question arises, what happens to Laplacian. As investigated in [13], the Laplacian converges in the norm resolvent sense to a 1-dimensional Schrödinger operator with an effective potential holding the information about the twisting/bending.

From this point of view we are able to effectively approximate the dynamics in the thin waveguide, hence we can suppose the heat equation (10) being in the one-dimensional form

$$u_t - u_{xx} + V(x)u = 0, \tag{13}$$

with $V = C_\omega \dot{\theta}^2$. Here C_ω depends on the cross-section ω and is identically zero if the cross-section is rotationally symmetric.

Definition 4. The self-similarity transformation is defined as

$$u(x,t) = (t+1)^{-1/4} w(y,s), \tag{14}$$

in the new coordinates y and s, where $y := (t+1)^{-1/2}x,\ s := \ln(t+1)$, so the meaning of y, respectively s, being spatial, respectively time coordinate, still stays on [7].

By applying the self-similarity transformation (14) to the heat equation (13) we get the expression

$$w_s - \frac{1}{2} y w_y - \frac{1}{4} w - w_{yy} + e^s V(e^{s/2} y) w = 0. \tag{15}$$

The self-similarity transformation is unitary in space variables:

$$\|u(t)\| = \|w(s)\|.$$

But this is not the end of the story- it is more comfortable to transform (15) by obeying

$$z(y,s) := e^{y^2/8} w(y,s). \tag{16}$$

After this transformation we come to the form

$$z_s - z_{yy} + \frac{y^2}{16} z + e^s V(e^{s/2} y) z = 0. \tag{17}$$

The complete proof of Theorem 3.1 is findable in [7], here we just sketch it to demonstrate the background behind the self-similarity theory.

Proof. Let us multiply (17) by z and then integrate by parts the expression with respect to y. We arrive at the equation

$$\frac{1}{2} \frac{d}{ds} \|z\|^2 + \langle z, H_s z \rangle = 0, \tag{18}$$

where

$$H_s := -\partial_{yy} + \frac{y^2}{16} + e^s V(e^{s/2}y). \tag{19}$$

The longitudinal part of H_s coincides with the quantum harmonic oscillator Hamiltonian

$$H := -\frac{d^2}{dy^2} + \frac{1}{16}y^2 \quad \text{in } L^2(\mathbb{R}). \tag{20}$$

From the Rayleigh-Ritz principle it follows that

$$\langle z, H_s z\rangle \geq \lambda_1(s)\|z\|^2, \tag{21}$$

where λ_1 is the time-dependent first eigenvalue of the operator H_s. By combining (18) and (21) we get

$$\frac{1}{2}\frac{d}{ds}\|z\|^2 \leq \lambda_1(s)\|z\|^2.$$

The solution is known:

$$\|z(s)\| \leq e^{-\int_0^s \lambda_1(\sigma)d\sigma}\|z(0)\|. \tag{22}$$

Therefore, if $V = 0$, (18) turns to Hamiltonian of harmonic oscillator in spatial coordinates, thus the first eigenvalue is $\lambda_1 = 1/4$ (as will be stated below). Plugging this into the equation (22) we get

$$\|z(s)\| \leq e^{-\frac{1}{4}s}\|z(0)\|.$$

As shown in Proposition 1. in [7], we may return to the original coordinates taking advantage of the weighted space properties. According to Corollary 1. in [7], the transition from the exponential to the polynomial decay rate is made. Indeed, the desired result is proved that $\gamma(\Omega_\theta) = 1/4$ if the waveguide is untwisted.

Summing up, if $V = 0$ then the heat equation via the harmonic oscillator solution is explicitly solvable and we found out that it behaves as $t^{-1/4}$, which conforms to the first eigenvalue of the oscillator.

The twisted case is more involved. Because $V \geq 0$, V is not identically equal to zero, in every time $\lambda_1(s) \geq 1/4$. Let us suppose we found the first eigenvalue $\lambda_1(s)$ of the operator H_s associated with the normalized eigenvector ψ_s:

$$\langle \psi_s, H_s\psi_s\rangle = \lambda_1(s)\|\psi_s\|^2 = \lambda_1(s). \tag{23}$$

The left-hand side can be altered by using the exact form of H_s from (19):

$$\langle \psi_s, H_s\psi_s\rangle = \|\dot{\psi}_s\|^2 + \left\|\frac{x}{4}\psi_s\right\|^2 + \int e^s V(e^{s/2}y)\psi_s^2(y)dy.$$

Firstly, we know from the minimax principle that for $\lambda_1(s)$ as the threshold energy $\forall\psi \in D(H_s)$ holds

$$\lambda_1(s) \leq \frac{\langle \psi, H_s\psi\rangle}{\|\psi\|^2}, \tag{24}$$

hence for the second eigenvector $\psi = \psi_2$ the right-hand side goes to the second eigenvalue $\lambda_2(s) = 3/4$ as $s \to \infty$. Indeed, the right-hand side of (24) is in the form

$$\left\langle \psi_2, \left(-\frac{d^2}{dy^2} + \frac{y^2}{16}\right) \psi_2 \right\rangle + \left\langle \psi_2, e^s V(e^{s/2}y)\psi_2 \right\rangle,$$

and while the first term coincides with the harmonic oscillator Hamiltonian and thus equals to $\lambda_2(s)$ (when ψ_2 normalized to 1), the second term is vanishing at the infinity according to (29), as listed below. As a consequence, $\lambda_1(s)$ has an upper bound which implies that (23) is also bounded. In particular, every term on the left-hand side of (23) must be bounded:

$$\|\dot{\psi_s}\| \leq C \tag{25}$$

$$\|x\psi_s\| \leq C \tag{26}$$

$$\int e^s V(e^{s/2}y)\psi_s^2(y)dy \leq C \tag{27}$$

Consequently, the condition (25) together with normalization $\|\psi_s\| = 1$ suggests that ψ_s is bounded in the Sobolev space H^1 as well: $\|\psi_s\|_{H^1} \leq C$. Which means that ψ_s weakly converges to ψ_∞ as $s \to \infty$ in H^1.

We recall the fact mentioned in [7] that the form domain of H

$$D(H^{1/2}) = H^1(\mathbb{R}) \cap L^2(\mathbb{R}, |x|^2 dx)$$

is compactly embedded in $L^2(\mathbb{R})$, so that the spectrum of H, consequently of H_s as well, is purely discrete. Indeed, according to Theorem XIII.64 in [10], the operator with compact resolvent has purely discrete spectrum and a complete set of eigenfunctions, i.e. there exists a complete orthonormal basis $\{\psi_n\}_{n=1}^{\infty}$ in $D(H_s)$ so that $H_s\psi_n = \lambda_n(s)\psi_n$ with $\lambda_1(s) \leq \lambda_2(s) \leq \ldots$ and $\lambda_n(s) \to \infty$ as $n \to \infty$. Also, $\{\lambda_n(s)\}_{n=1}^{\infty}$ has no finite accumulation point.

Thus, the eigenvectors converge even in the strong sense:

$$\psi_s \xrightarrow{s} \psi_\infty, \text{ in } L^2(\mathbb{R}). \tag{28}$$

The third condition (27) obeys

$$e^{s/2} \int V(e^{s/2}y)\, dy\, |\psi_s|^2 \leq Ce^{-s/2}. \tag{29}$$

The right-hand side of (29) goes to 0 as $s \to \infty$.

The Dirac delta interaction may be expressed as a limit in the distributional sense by

$$\frac{1}{\varepsilon}V\left(\frac{x}{\varepsilon}\right) \xrightarrow{\varepsilon \to 0} \delta(x) \int V(x)dx. \tag{30}$$

Distributions, also called *generalized functions*, are essentially functionals. The Dirac delta function δ as an example of distributions was defined in a very rough way as a function that was 0 for every x except $x = 0$ and was infinite at $x = 0$

in such a way that the integral $\int_{-\infty}^{\infty} \delta(x)dx = 1$. Of course, there is no such function, the definition in the words of distributions yields

$$\delta(\varphi) = \langle \delta, \varphi \rangle = \varphi(0), \tag{31}$$

setting φ a test function.

All in all, plugging (28) (and taking consequences of (31)) and (30) into (29) we arrive at the limit inequality

$$\int V(y)\, dy\, |\psi_\infty(0)|^2 \leq 0,$$

since V is non-negative, we can conclude with

$$\psi_\infty(0) = 0. \tag{32}$$

So clearly the potential scalling is more singular than the Dirac Δ-interaction scalling, which leads to Dirichlet condition at the origin of coordinates in the long-times limit. This problem of the harmonic oscillator with Dirichlet condition is already explicitly solvable. More specifically:

Let $\phi \in C_0^\infty(\mathbb{R}\backslash\{0\})$ be arbitrary. Then taking it as a test function in (19) (the brackets are not anymore arranged in the weighted space but in $L^2(\mathbb{R})$) we set:

$$\langle \dot{\phi}, \dot{\psi_s} \rangle + \langle \phi, \frac{x^2}{16}\psi_s \rangle + \int \phi e^s V(e^{s/2}y)\psi_s\, dy = \lambda_1(s) \int \phi\psi_s\, dy.$$

Sending s to infinity and taking use of (32) we arrive at

$$\langle \dot{\phi}, \dot{\psi_\infty} \rangle + \langle \phi, \frac{x^2}{16}\psi_\infty \rangle = \lambda_1(\infty)\langle \phi, \psi_\infty \rangle.$$

In particular, $\lambda(s)$ converges to the first eigenvalue of H with Dirichlet condition at $x = 0$ as $s \to \infty$ which coincides with the second eigenvalue of H, in the view of symmetry. This conforms to

$$\lambda(\infty) := \lim_{s\to\infty} \lambda(s) = \frac{3}{4}.$$

$\square$

The advantage of (17) lies in the compactness of the resolvent of the operator, while the dependence of the potential on time is not convenient at all. We can interpret the consequence of Theorem 3.1 as that since $V = 0$ in the untwisted case, the norm of the solution of the heat equation $\|u(t)\| \sim t^{-1/4}$, however for $V \geq 0, V \neq 0$ in the twisted case, the decay rate gains a further increment at least $1/2$ and the solution norm is estimated from upper as

$$\|u(t)\| \leq C_\varepsilon \|u_0\|_K e^{-E_1 t} t^{-(3/4-\varepsilon)}$$

for arbitrary small ε.

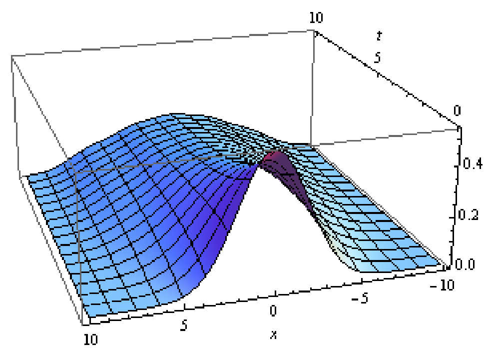

Figure 3: Time evolution of the heat equation solution

4 Numerical results

The analytical results are due to the article [7] well-known, but the numerical confirmation is still missing. We used the Wolfram Mathematica 7.0 and MATLAB R2010a environment to support the data given by David Krejčiřík and Enrique Zuazua. For the untwisted one-dimensional problem we know the exact solution hence the comparison of used methods is available. All three methods utilized below are rewritten in their Mathematica code in Appendix.

4.1 Untwisted case

4.1.1 Exact solution in one-dimensional case

The solution of the heat equation (13) with $V = 0$ on the string is analytically known. The derivation of the fundamental form is available in [4], the following Green's function solution is recorded there:

$$u(x,t) = \int_{\mathbb{R}} G(x,y,t) u_0(y) dy, \tag{33}$$

where the Green's heat kernel is defined

$$G(x,y,t) = \frac{e^{-\frac{|x-y|^2}{4t}}}{\sqrt{4\pi t}}.$$

We are thus able to numerically compute the time evolution of some initial state as well as the asymptotical norm behaviour. More importantly, we can use this exact solution for comparing the other methods in order to pick out the most suitable of them also for the case the solution is not exactly findable anymore.

Mathematical model of (33) evolution with the first eigenfunction of the harmonic oscillator as the initial state is evolved in Mathematica environment on the Figure 3.

4.1.2 Solution via eigenbasis decomposition

The equation (13) with $V = 0$ a bit admonish of about the harmonic oscillator Hamiltonian. Hence, the first way how to numerically solve it without knowing the exact solution is via the oscillator eigenbasis decomposition. The Ansatz is imposed:

$$u(x,t) = \sum_{n=1}^{\infty} a_n(t)\psi_n(x). \tag{34}$$

ψ_n satisfies the stationary Schrodinger equation with the harmonic oscillator potential $-\psi_n'' + \frac{x^2}{16}\psi_n = \lambda_n\psi_n$, from quantum mechanics (findable for instance in [11]) we know the exact expression of the eigenvectors and eigenvalues:

$$\lambda_n = \frac{1}{2}\left(n + \frac{1}{2}\right), \qquad \psi_n(x) = \mathcal{N}_n H_n\left(\frac{x}{2}\right)e^{-\frac{x^2}{8}},$$

in the coordinates where $\omega = m = 1/2, \hbar = 1$ and where H_n is the Hermite polynomial.

When (34) applied to (13) we arrive at

$$a(t) = e^{-Mt}a(0),$$

where

$$M_{mn} = \lambda_n\delta_{mn} - \left\langle \psi_m, \frac{x^2}{16}\psi_n \right\rangle.$$

By setting the initial condition as $u_0(x) = \psi_0(x)$, we are able to find the numerical solution in Mathematica, before we compare this method with the exact solution, we propose a third method, the self-similarity transformation defined above.

4.1.3 Solution via self-similarity transformation

Let us attempt to find a solution in the fashion of self-similarity transformation. Let us recall the transformed heat equation (17) without potential. The initial condition $u_0(x) = \psi_0(x)$ has to be transformed as well; then the new constants $a_n(0)$ satisfy the prescription

$$a_n(0) = \int \psi_{n-1}(x)\,\psi_0(x)\,e^{x^2/8}\,dx. \tag{35}$$

The solution of $z_s - z_{yy} + \frac{y^2}{16}z = 0$ may be again found in the form of harmonic oscillator decomposition (34). After some algebra we end up with

$$a(t) = e^{-Mt}a(0),$$

where

$$M_{mn} = \lambda_n\delta mn$$

which is possible to be computed via Mathematica and then re-transformed in the original units again.

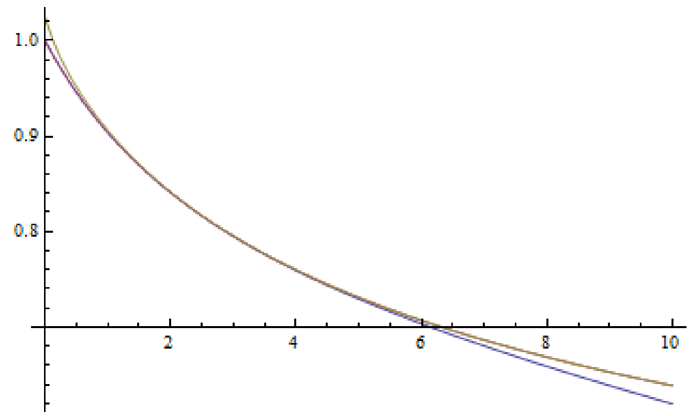

Figure 4: Time evolution of $\|u\|$ in the exact [violet], oscillator [blue] and self-similarity case [grey].

4.1.4 Comparison

The exact solution allows us to compare the preceding methods. To get more information about the asymptotics let us define a new quantity q which coincides with the decay rate (12):

$$q(t) := -\frac{\ln \|u(t)\|}{\ln (1+t)}. \tag{36}$$

When evolving $\|u(t)\|$ one get the result shown in Figure 4. Here the violet line denotes the exact solution, the blue line the solution via harmonic oscillator eigenbasis expansion and the grey one the solution via self-similarity transformation. One can easily see the diference between these three methods- while the blue case coincides with the exact solution at small times, the self-similarity solution is very inaccurate near the origin, actually, the solution at time $t = 0$ is not even normalized to 1 anymore. On the other side- the grey line is merging with exact solution as time goes to infinity, however, the violet line deviates more and more.

Indeed, by the same time the limit of the exact decay rate is $1/4$ as well as in the self-similarity case, the decay rate in the solution via oscillator eigenbasis diverges, however. This was proved numerically as well. Another confirmation of such behaviour gives the Figure 5 where the divergence of the rate in the oscillator case is obvious. The two lines- exact solution and the self-similarity case, coincide.

As a conclusion we can state that in spite of being suitable at small times, the harmonic oscillator eigenbasis expansion method fails as time increases. The opposite statement holds true for the self-similarity transformation, thus the latter method is more useful for asymptotical times in which we are interested.

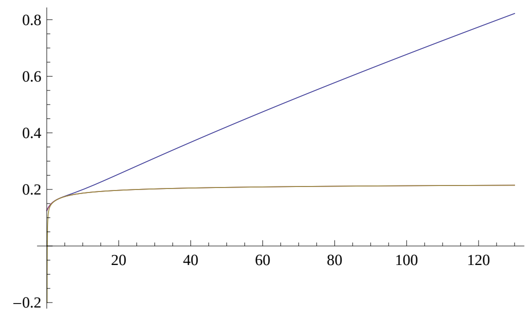

Figure 5: Time evolution of the decay rates in the exact [violet], oscillator [blue] and self-similarity case [grey].

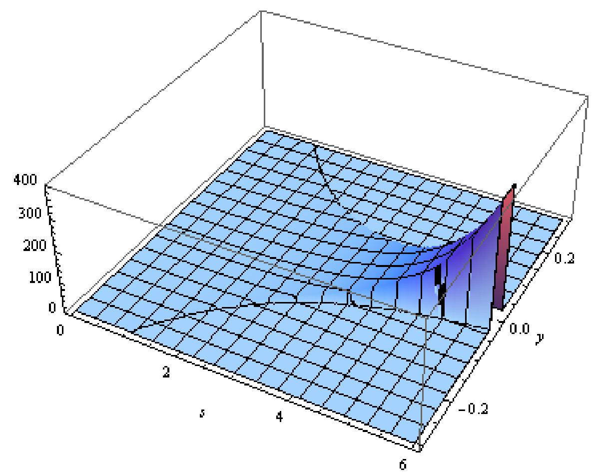

Figure 6: Scalled potential evolution. The thicker, the higher.

4.2 Twisted case

As we already know from the analytical part, the potential V which is not identically equal to zero increases the decay rate about $1/2$. Mathematically, the background lies in scalling which is more singular than the Dirac's delta interaction and thus leads to the Dirichlet condition at the origin. To illustrate this statement, the scalled potential V is to seen on Figure 6. As the support is getting thicker, the peak is getting higher.

This problem is already explicitly solvable: the first eigenvalue is $3/4$, which coincides with the second eigenvalue of the harmonic oscillator without Dirichlet condition.

To show this numerically we carry out the method of self-similarity transformation which is more accurate for asymptotical times, as was proved above. Thus we come out from the transformed equation (17). Two slightly different approaches are utilized. In the first case the Ansatz (34) is used, in the second case the direct counting command `NDSolve` is applied.

Let us start with the oscillator eigenbasis expansion. The same approach for transforming the initial condition as in (35) is utilized. Then (17) gets the form

$$\sum_n (\dot{a_n} + a_n\lambda_n + e^s V(e^{s/2}y)\, a_n)\, \psi_n = 0, \tag{37}$$

where λ_n are the eigevalues of the harmonic oscillator Hamiltonian (20). Henceforth, for numerical computations we simply consider the potential V, which simulates the twist, being a unit box:

$$V(x) = \begin{cases} 1 & \text{if } x \in [-1,1] \\ 0 & \text{otherwise.} \end{cases} \tag{38}$$

Then by applying (38) to (37), multiplying the whole expression with ψ_m and integrating with respect to y we get the formula

$$\dot{a_m} + a_n\lambda_n\delta_{mn} + \sum_n e^s \int_{-e^{-s/2}}^{e^{-s/2}} a_n\psi_n\psi_m \, dy = 0.$$

This system of equations is solved in the Mathematica environment with help of the predefined command `NDSolve`. With the view of the computational duration we considered $n = 9$.

Is spite of the resulting plot seeming to behave stable in the asymptotic times, the decay rate isn't approaching the correct limit. For all the initial conditions and different integers n of eigenvectors in the expansion, the decay rate in the twisted case increased more rapidly then in untwisted case, but we were not able to show the asymptotic behaviour as stated in the crucial article [7].

The second approach gives slightly better results. We compute directly the transformed equation (17) with the command `NDSolve`. The initial state is not anymore expanded to the eigenbasis and we directly employ (14) and (16). Thus we arrive at the transformed initial condition

$$z_0(y) := \psi_0(y)\, e^{y^2/8}.$$

Then the re-transformed solution of the heat equation in the twisted waveguide is plotted on the Figure 7.

On the Figures 8 and 9 you may see the norm evolution and decay rate in comparison to the untwisted case. As obvious, the norm is decaying more sharply where the step-like potential is imposed. The decay rate seems to be satisfactorily tending to 3/4 as was prescribed. Unfortunately, the time is not asymptotical and the program is really unstable for larger times. Moreover, it is also very much ill-conditioned, depending on the initial conditions, which means that the given results despite looking like precise may not be taken as proof for the statement given in [7].

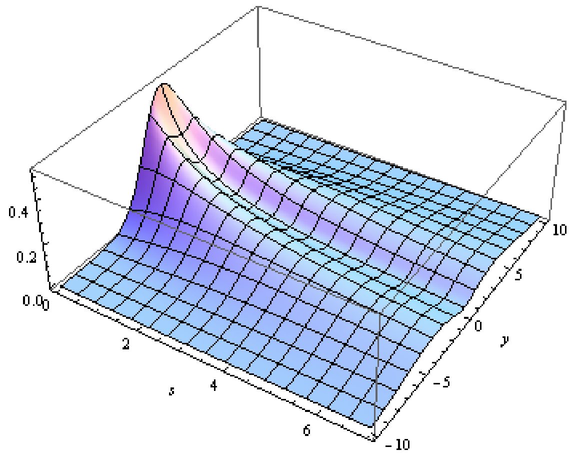

Figure 7: Solution of the heat equation with a step-like potential.

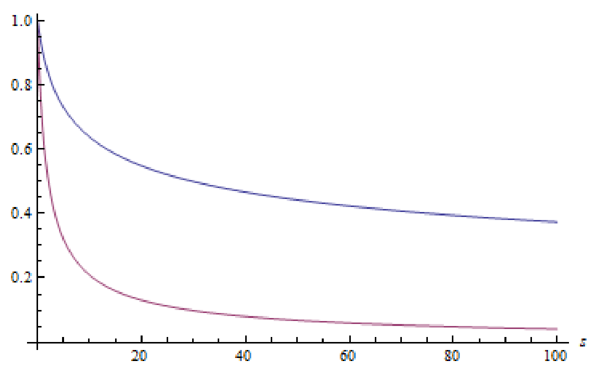

Figure 8: The norm evolution comparison in the untwisted (blue) and twisted (violet) case.

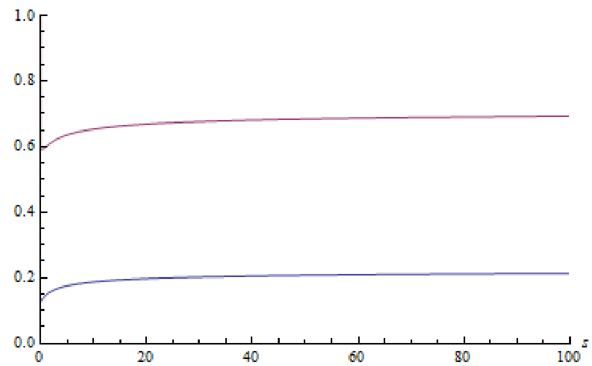

Figure 9: Decay rate in the untwisted (blue) and twisted (violet) case.

4.3 Spectral methods

At last but not at least, the task also included the spectral method and its usage in MATLAB. Spectral methods are one of the techniques successfully used to numerically solve certain partial differential equations which provide an alternative to finite difference or finite element methods.

Where applicable, spectral methods can achieve the fastest convergence, for problems with simple domains and smooth solutions the spectral methods are the best tool. The error decreases very rapidly and this behaviour is called *spectral accuracy.* It is confirmed by both the theory and the numerical experience. While the error in a finite difference or finite element methods decreases as $O(N^{-m})$ for some constant m as N increases, for a spectral method, convergence at the rate $O(N^{-m})$ for *every* m is achieved and even faster convergence at a rate $O(c^N)$ $(0 < c < 1)$ is achieved if the solution is analytic [14].

As we made ourselves familiar with spectral methods we are able to apply them on solution of the heat equation (1). We successively solved the series of problems:

- 1D finite interval
- 2D finite rectangle

4.3.1 One-dimensional interval

Let us consider the heat equation on finite interval $[-\pi, \pi]$ with the boundary conditions

$$a_1 u(1) + b_1 u'(1) = c_1, \quad a_N u(-1) + b_N u'(-1) = c_N,$$

where N is the number of points rescalled to the interval, and a_i, b_i, c_i are some real constants for $i = 1, 2$. The Dirichlet conditions respond to the case

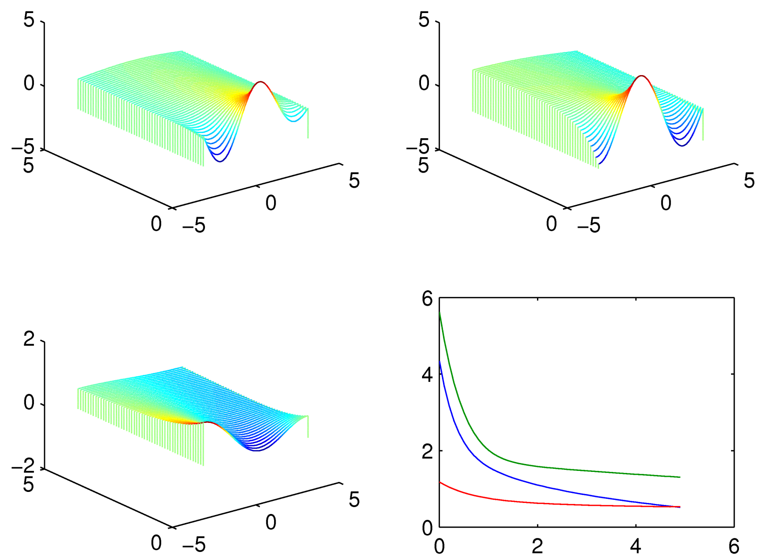

Figure 10: Time evolution of the heat equation with a) DD b) ND c)NN boudary conditions. L^2-norm.

$a_1 = a_N = 1$, $b_1 = b_N = c_1 = c_N = 0$. Numerican computation follows the theoretical prescription in the semigroup fashion (9) with

$$u_0(x) = \cos(x/2) + 2\cos(3x/2) + \sin(x)$$

as the initial state. The result is introduced on Figure 10, at the first subfigure.

The second subfigure presents the Neumann-Dirichlet case. Here the boundary conditions are $a_1 = b_N = 1$, $b_1 = c_1 = a_N = c_N = 0$. We choose initial state as

$$u_0(x) = \cos((x+\pi)/4) - \cos(3(x+\pi)/4)/5 - 3\cos(5(x+\pi)/4).$$

We take adventage from ready-made MATLAB programes `chebdif` and `cheb2bc` by S. C. Reddy, J. A. C. Weideman which are free available in http://dip.sun.ac.za/ weideman/research/differ.html.

The Neumann-Neumann condition is embeded similary as in previous case, the only difference is in taking $b_1 = b_N = 1$, $a_1 = c_1 = a_N = c_N = 0$ and

$$u_0(x) = 1/5 - \sin(x/2)/3 - \cos(x)/2$$

as the initial state.

The last subfigure of Figure 10 shows the decrease of L^2-norms in the previous problems. The blue line denotes the DD-case, the most rapidly decreasing green line denotes the DN-case, the red one is the NN-case. The initial states are chosen as a finite linear combinations of solutions of the stationary Schrödinger equation on the finite interval with given boundary conditions.

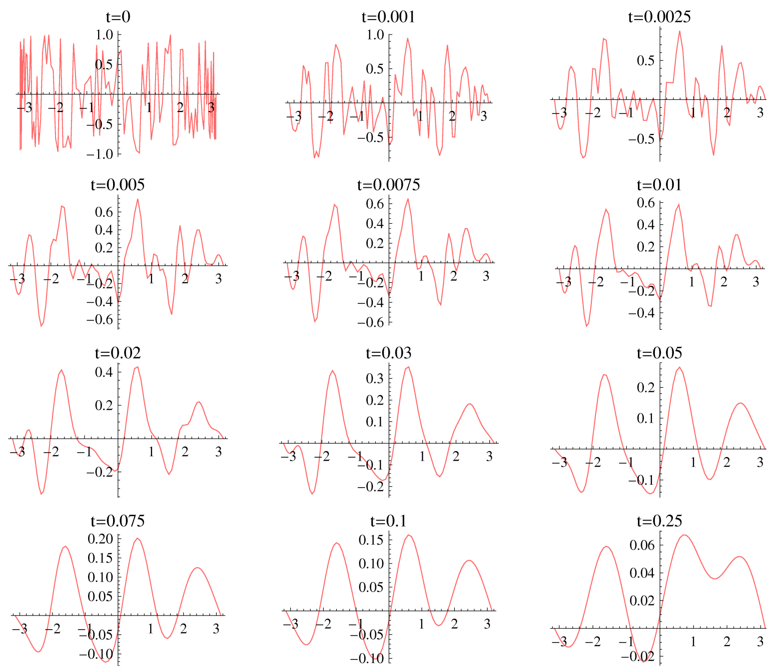

Figure 11: White noise, short-time evolution.

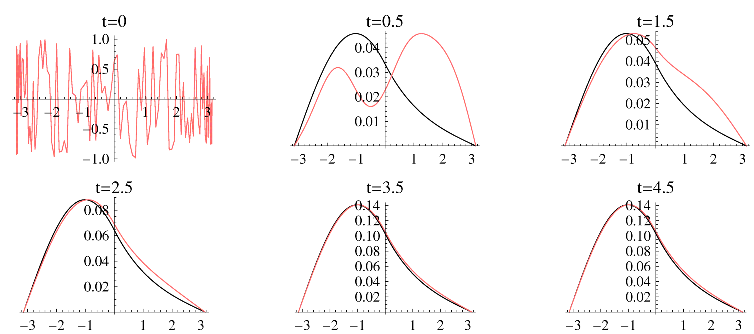

Figure 12: White noise, long-time evolution.

There is also another advantage of $u(x)$ being expressed in the semigroup form (9), namely the generality of such formula. For instance, let us set a random function, so-called *white noise*, as the initial state and evolve it in time. After some time the randomness disappears and the function is getting closer to the first eigenvector of the operator. This behaviour is illustrated on the Figure 11 and Figure 12.

On Figure 11 you can see the short-time evaluation. The initial function is getting smoother and waver to the first eigenvector. On Figure 12 the long-term effects are shown. In $t = 4.5$ the white noise almost coincides with the first eigenvector of the operator (here denoted by the bold line), thus the influence of the first eigenvalue in the semigroup operator $e^{-\Delta t}$ is crucial.

4.3.2 Two-dimensional finite rectangle

In the 2D computations we naturally set up a grid based on grid points independently in each direction, called a *tensor product grid*, where the great majority of points lie near the boundary. Let us firstly consider a finite rectangle $(-a, a) \times (-b, b)$ with the Dirichlet and Neumann boundary condition on the lines (see Figure 2a). The twist of the waveguide is realized as a switch of the boundary conditions in one point (Figure 2b).

A ready-made application `herdif` again by J.A.C Weideman and S.C. Reddy, which computes the differentiation matrices up to given order, is uploaded. In the transversal direction the boundary conditions are changing with x-coordinate, what we have to count with. Then again `cheb2bc` function is used. As a result we can see the Figure 13 where the first four eigenvalues with the countour plot of such problem are plotted.

Finally, the moving frame is presented on the webpage. Here, the time evolution of heat equation in finite twisted rectangle is performed. The initial condition is chosen as $v_0 = v_2 + 3v_4 - 2v_3$ and one can graphically see the norm decay. Advice- to see the frame moving one should open the pdf file in Acrobat Reader, not by the build-in Google docs pdf converter.

5 Conclusion

In the research work we were concerned with the asymptotical properties of the decay rate of the heat equation semigroup. Firstly, we introduced twisted waveguides and heat equation and defined the self-similarity transformation which plays an important role in modeling of the asymptotical behaviour. Further, we were interested in the decay rate as a measurement of the decay. As proved in [7] the decay rate is about 1/2 greater in the twisted than in the untwisted case. Our aim was to numerically support this data and thereby complete the article, where analytical approach has been reached. The last chapter is devoted to numerical modeling of described situations.

The motivation for the present work was to get familiar with some up-to-date results in the waveguide theory as well as with the numerical methods

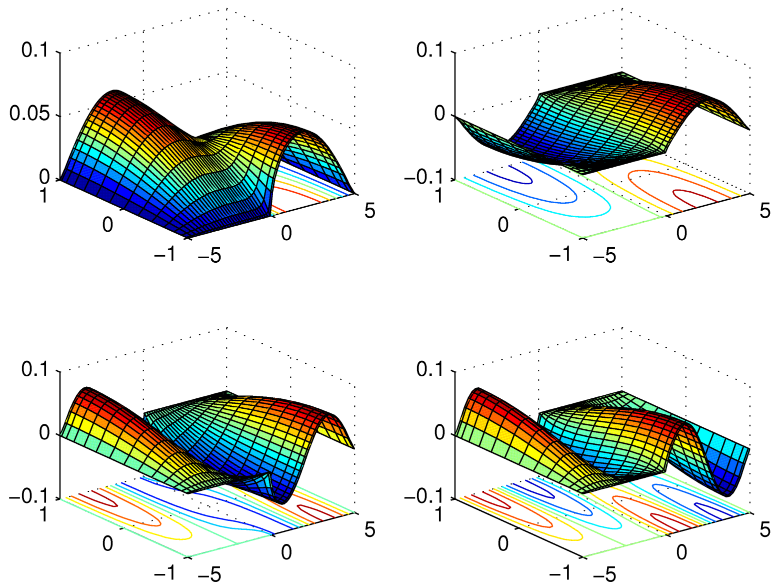

Figure 13: Eigenvectors of the twisted 2D case.

useful in such computations, above all the spectral method. The results are unfortunately not sufficiently conclusive, the developed methods are unstable and ill-conditioned. It is however obvious, that in the twisted case the decay rate is greater in the untwisted waveguide.

Some numerical results related with the topic are presented as a introduction to the spectral methods.

The desirable aim how to extend the work lies of course in evolving more precise numerical method which would be more stable. Another possible goal is to provide a computation for non-approximated 3D waveguides, not only for those introduced through the effective potential.

This work freely follows-up present author's bachelor thesis [9] where the influence of twisting of a quantum waveguide on the free particle's Hamiltonian spectrum has been investigated.

Appendix

The source code for Wolfram Mathematica

In this section we provide the source code for the numerics in Wolfram Mathematica 7.0. Three methods for solving heat equation without potential, i. e. the untwisted case, are provided here. The decay rate in all the cases is computed below.

```
(*preliminaries: eigenfunctions of the harmonic oscillator *)

psi[n_, x_] = Sqrt[1/(2^n * n!)] * (1/4/Pi)^(1/4) * E^(-x^2/8) * HermiteH[n, x/2]

(* solution via the heat kernel *)

p[t_, x_, y_] = E^(-(x - y)^2/4/t)/Sqrt[4 * Pi * t]
uexact[t_, x_] = Integrate[p[t, x, y] * psi[0, y], {y, -Infinity, Infinity},
Assumptions → {t > 0}]
normuexact[t_] =
Sqrt[Integrate[uexact[t, x]^2, {x, -Infinity, Infinity}, Assumptions → {t > 0}]]

(* solution via expansion of the solution into the eigenbasis of the harmonic oscillator*)

Clear[range]; range = 10;
m = Table[(n - 1 + 1/2)/2 * KroneckerDelta[m, n]-
Integrate[psi[m - 1, x] * x^2/16 * psi[n - 1, x], {x, -Infinity, Infinity}],
{m, 1, range}, {n, 1, range}];
expm[t_] = MatrixExp[-m * t];
a0 = Table[If[n == 1, 1, 0], {n, 1, range}];
a[t_] = expm[t].a0;
u[t_, x_] = Sum[a[t][[n]] * psi[n - 1, x], {n, 1, range}];
normu[t_] =
Sqrt[Integrate[u[t, x]^2, {x, -Infinity, Infinity}, Assumptions → {t > 0}]];

(*solution via expansion of the self-similar solution into the eigenbasis of the harmonic oscillator *)

Clear[range]; range = 5;
ms = Table[(n - 1 + 1/2)/2 * KroneckerDelta[m, n], {m, 1, range}, {n, 1, range}];
expms[s_] = MatrixExp[-ms * s];
a0s = Table[Integrate[psi[n - 1, x] * psi[0, x] * E^(x^2/8),
{x, -Infinity, Infinity}], {n, 1, range}];
as[s_] = expms[s].a0s;
```

```
ws[s_, y_] = Sum[as[s][[n]] * psi[n - 1, y], {n, 1, range}];
us[t_, x_] = (t + 1)^(-1/4) * ws[Log[t + 1], (t + 1)^(-1/2) * x]*
E^(-(t + 1)^(-1) * x^2/8);
normus[t_] =
Sqrt[Integrate[us[t, x]^2, {x, -Infinity, Infinity}, Assumptions → {t > 0}]];

rateexact[t_] = -Log[normuexact[t]]/Log[1 + t];
rate[t_] = -Log[normu[t]]/Log[1 + t];
rates[t_] = -Log[normus[t]]/Log[1 + t];
```

References

[1] J. Blank, P. Exner, M. Havlíček, *Lineární operátory v kvantové fyzice*, Univerzita Karlova, vydavatelství Karolinum, Praha (1993).

[2] P. Duclos and P. Exner, *Curvature-induced bound states in quantum waveguides in two and three dimensions*, Rev. Math. Phys. **7**, 73-102 (1995).

[3] T. Ekholm, H. Kovařík and D. Krejčiřík, *A Hardy inequality in twisted waveguides*, Arch. Ration. Mech. Anal. **188**, No. 2, 245-264 (2008).

[4] L. C. Evans, *Partial differential equations*, Graduate Studies in Mathematics, Berkeley (1997).

[5] P. Exner and P. Šeba, *Bound states in curved quantum waveguides*, J. Math. Phys. **30**, 2574-2580 (1989).

[6] D. Krejčiřík, *Twisting versus bending in quantum waveguides*, Proc. of Symp. in Pure Math. **44** (2008), 617-636.

[7] D. Krejčiřík, E. Zuazua, *The asymptotic behaviour of the heat equation in a twisted Dirichlet-Neumann waveguide*, J. Differential Equations **250** (2011), 2334-2346.

[8] D. Krejčiřík, E. Zuazua, *The Hardy inequality and the heat equation in twisted tubes*, J. Math. Pures Appl. **94** (2010), 277-303.

[9] G. Malenová, *Quantitative Study of Hardy Inequalities in Twisted Waveguides*, Bachelor thesis, supervisor D. Krejčiřík, CTU in Prague (2010).

[10] M. Reed, B. Simon, *Methods of modern mathematical physics, IV. Analysis of operators*, Academic Press, New York (1978).

[11] H.C. Rosu, *Elementary Nonrelativistic Quantum Mechanics*, arXiv:physics/0004072v2, Los Alamos Electronic ArXives, (2000).

[12] R. E. Showalter, *Monotone Operators in Banach Space and Nonlinear Partial Differential Equations*, American Mathematical Society, (1997).

[13] H. Šediváková, *Quantum Waveguides under Mild Regularity Assumptions*, Diploma thesis, supervisor D. Krejčiřík, CTU in Prague (2011).

[14] L. N. Trefethen, *Spectral Methods in MATLAB*, SIAM, Philadelphia (2000).